Journal of Stored Products Research 99 (2022) 102031

Contents lists available at ScienceDirect

Journal of Stored Products Research

journal homepage: www.elsevier.com/locate/jspr

Non-thermal plasma as emerging technology for *Tribolium castaneum* pest-management in stored grains and flours

Carla Zilli [a,b,*], Nicolás Pedrini [c], Eduardo Prieto [d], Juan Roberto Girotti [c], Pablo Vallecorsa [a], Matías Ferreyra [e], Juan Camilo Chamorro [e], Ezequiel Cejas [e], Brenda Fina [e], Leandro Prevosto [e], Karina Balestrasse [a,b,**]

[a] *Instituto de Investigaciones en Biociencias Agrícolas y Ambientales (INBA), Facultad de Agronomía, Universidad de Buenos Aires (UBA), Consejo Nacional de Investigaciones Científicas y Técnicas (CONICET), Buenos Aires, Argentina*
[b] *Cátedra de Bioquímica, Departamento de Biología Aplicada y Alimentos, Universidad de Buenos Aires, Facultad de Agronomía, Buenos Aires, Argentina*
[c] *Instituto de Investigaciones Bioquímicas de La Plata (INIBIOLP), CCT La Plata Consejo Nacional de Investigaciones Científicas y Técnicas (CONICET), Universidad Nacional de La Plata (UNLP), La Plata, Argentina*
[d] *Instituto de Investigaciones Fisicoquímicas Teóricas y Aplicadas (INIFTA) (CCT LA PLATA). Departamento de Cs. Biológicas, Facultad de Ciencias Exactas (UNLP), Instituto Ciencias de la Salud, Universidad Nacional Arturo Jauretche (UNAJ), Argentina*
[e] *Universidad Tecnológica Nacional, CONICET, Facultad Regional Venado Tuerto Departamento Ing. Electromecánica, Grupo de Descargas Eléctricas (GDE), Laprida 651, Venado Tuerto, 2600, Argentina*

ARTICLE INFO

Keywords:
Plasma technology
Pest management
Tribolium castaneum
Oxidative stress
Atomic force microscopy

ABSTRACT

The red flour beetle, *Tribolium castaneum* (Herbst) (Coleoptera: Tenebrionidae), is a major secondary pest on wheat stored in metal bins, silo-bags and is also frequently found in wheat products such as flour. Non-thermal plasmas (NTPs) are (quasi-neutral) partially ionized gases that may be produced by a variety of electrical discharges. We propose the use of an atmospheric pressure dielectric barrier discharge (DBD) as an emerging technology in post-harvest integrated pest management. To this aim, a series of experiments were performed in order to test the lethality of such plasmas on three life stages of *T. castaneum* by measuring insect mortality and their impacts on physiological and biochemical parameters affecting insect fitness. The different NTP treatments were performed by increasing the time of exposure to either O_2 or N_2 used as carrier gases. After 24 hours, high levels of mortality (30–100%) were reached for each applied treatment, in both larval and adult populations. Mortality seems to be related to a significant water content loss and redox imbalance. Atomic force microscopy (AFM) scanning of the prothoracic surface showed that nitrogen causes more severe damage than oxygen. As a consequence of the cuticle damage, the quinone-containing secretions of the prothoracic and abdominal glands were affected. We also carried out experiments on egg-containing flours to test the ovicidal activity of NTP. The flours were evaluated at three and twelve weeks after treatments. A 3-min nitrogen treatment showed ovicidal properties, while the remaining NTPs partially killed the eggs and delayed the emergence of larvae and adults. In conclusion, we propose an inexpensive physical treatment, which controls the entire life cycle of a major grain pest, avoiding chemical residues.

1. Introduction

During grain storage, it is important to maintain conditions that minimize grain losses due to physical, chemical and biological agents. The principal causes of spoilage in stored grain are fungi, insects and mites. Therefore, major efforts are often undertaken to prevent colonization and growth of these organisms. The red flour beetle, *Tribolium castaneum* (Herbst) (Coleoptera: Tenebrionidae), is a major secondary pest on wheat stored in metal bins, silo bags and mills. It is also frequently found in wheat-based products such as flour and pasta at

* Corresponding author. Instituto de Investigaciones en Biociencias Agrícolas y Ambientales (INBA), Facultad de Agronomía, Universidad de Buenos Aires (UBA), Consejo Nacional de Investigaciones Científicas y Técnicas (CONICET), Buenos Aires, Argentina.
** Corresponding author. Instituto de Investigaciones en Biociencias Agrícolas y Ambientales (INBA), Facultad de Agronomía, Universidad de Buenos Aires (UBA), Consejo Nacional de Investigaciones Científicas y Técnicas (CONICET), Buenos Aires, Argentina.
E-mail addresses: czilli@agro.uba.ar (C. Zilli), kbale@agro.uba.ar (K. Balestrasse).

https://doi.org/10.1016/j.jspr.2022.102031
Received 16 June 2022; Received in revised form 15 September 2022; Accepted 19 September 2022

warehouses and retail stores.

Chemical pesticides and fumigants are used extensively to control insects in stored grain facilities, but they are under increasing restrictions due to their environmental impact, residual toxicity and pesticide resistance. In particular, *T. castaneum* has developed resistance against commonly used chemical compounds like phosphine (Gautam et al., 2016; Jagadeesan et al., 2012) and deltamethrin (Singh and Prakash, 2013). Moreover, synthetic pesticides cannot be applied directly to processed foods or surfaces that contact food, thus processors depend more on alternative control methods. Therefore, recent efforts have focused on different physical and biological strategies in pest management science. Regarding biological control, the insecticidal activity against *T. castaneum* of the bioactive plant essential oils (Saroukolai et al., 2010; Sahaf et al., 2007) has been reported. Many other natural compounds, including mustard and coconut, were also tested (Khanzada et al., 2015).

Yang et al. (2009) designed nanoparticles loaded with garlic essential oil to evaluate their insecticidal activity against *T. castaneum*. Among these non-chemical insect control methods, the use of entomopathogenic fungi was also proposed (Hajek and St. Leger, 1994). *Metarhizium anisopliae* (Metschnikoff) Sorokin and *Beauveria bassiana* (Balsamo) Vuillemin showed activity against a broad range of insects. However, some authors reported that adult populations of *T. castaneum* were tolerant to *B. bassiana* (Akbar et al., 2004; Lord, 2007). In an attempt to understand the basis of this behavior, Pedrini et al. (2015) provided a molecular mechanism involving two cuticular secretions, methyl-1,4-benzoquinone (MBQ) and ethyl-1,4-benzoquinone (EBQ), and a fungal detoxifying enzyme as key components.

On the other hand, UV radiation (Faruki et al., 2007; Khan et al., 2021), microwaves and ozone treatments (Holmstrup et al., 2011; McDonough et al., 2011; Patil et al., 2020; Xinyi et al., 2017) were assayed as potential tools for pest management. Among these procedures, non-thermal plasmas (NTPs) emerge as a promising strategy for physical control of pests. NTPs allowed high mortality ratio under less than 1 min exposure, compared with the several minutes reported for UV-treatments, or hours, in the case of ozone treatments.

Atmospheric pressure non-thermal plasmas are (quasi-neutral) partially ionized gases that may be produced by a variety of electrical discharges (Bruggeman et al., 2017; Fridman et al., 2005). Among the variety of NTP sources, the dielectric barrier discharges (DBDs) are self-sustaining electrical discharges in electrode configurations containing an insulating material (the so-called dielectric barrier) in the discharge path. This is responsible for a self-pulsing plasma operation and thus, the formation of a non-thermal plasma at atmospheric pressure (Brandenburg, 2017). The basic feature of these various technologies is that they produce plasmas in which the majority of the electrical energy primarily goes into the production of energetic electrons, instead of heating the entire gas stream. These energetic electrons produce excited species (free radicals and metastable states) as well as additional electrons through electron-impact dissociation, excitation and ionization of background gas molecules. Due to these unique features, atmospheric pressure NTPs have found widespread use in a variety of industrial applications such as pollution control applications, volatile organic compounds removal, car exhaust emission control and polymer surface treatment (Kunhardt, 2000); and more recently, also in biological applications, ranging from inhibition of clinical fungi growth (Daeschlein et al., 2014), through food decontamination and food processing surfaces (Dasan et al., 2016; Sen et al., 2012) to agriculture (Adamovich et al., 2022). Previous studies were focused on the fungicidal properties of NTP produced by DBDs on the *Diaporthe/Phomopsis* (D/P) complex, one of the most harmful group of fungal pathogens that colonize the inside of soybean seeds (Pérez-Pizá et al., 2021; 2019). Those works showed that in addition to the efficiency of NTP treatments in controlling the D/P complex, seed viability and plant development were preserved.

Only a few studies have investigated the NTP technology for the pest-management in recent years (Donohue et al., 2015; Hassan et al., 2020; Ratish Ramanan et al., 2018; Ziuzina et al., 2021). This lack of scientific activity hampers the progress in the field. Furthermore, most of those experiments use low-pressure plasmas (Hassan et al., 2020; Ratish Ramanan et al., 2018) or expensive gases such as helium or argon (Donohue et al., 2015; Hassan et al., 2020) which limit them in several practical applications. Besides, compared to helium or argon plasma, air plasmas contain more active species that play a very important role in agriculture (Adamovich et al., 2022). However, the number of works dealing with atmospheric pressure air NTPs for pest control is scarce (Ziuzina et al., 2021). Our work sought to address such a knowledge gap.

The present work focuses on the effects of atmospheric pressure air NTP on different life stages of *T. castaneum*. As atmospheric pressure NTPs do not require expensive vacuum systems, this technology can be a cost-effective alternative to other non-conventional tools for pest management as microwave or low-pressure NTPs. We compared the effect of two different carrier gases produced by our plasma source on different stages of *T. castaneum*; i.e. eggs, larvae, and adults. Specifically, we performed mortality bioassays, we analyzed the plasma-induced damage on the cuticle surface of adults by atomic force microscopy (AFM), and the alterations of chemical secretion in adults by solid phase microextraction coupled to capillary gas chromatography (SPME-CGC). Also, we tested a redox imbalance as a potential cause of these alterations in the beetle life cycle.

2. Material and methods

2.1. Insects and rearing conditions

The *T. castaneum* insects were obtained from the Biochemistry Research Institute of La Plata (INIBIOLP). For this study, the stock culture was reared on wheat flour in plastic containers under dark conditions at 28 °C and 70% relative humidity. Every 5–6 days, adults were sieved and transferred to new recipients and fresh flour. Larvae were removed 3–4 weeks later using 500 μm sieves and transferred to new containers. Adult beetles of 2–4 weeks old used in the tests were of mixed-sex.

All life stages were reared on flour purchased from the local market. Upon arrival to the lab, it was frozen for 72 h to kill any residual eggs.

2.2. Plasma source and treatments

A schematic of the experimental setup is presented in Fig. 1. Briefly, it consisted of a DBD with a needle-array high-voltage electrode (with an overall diameter of 135 mm) and a plate ground electrode covered by a dielectric barrier of 1–4 polyester films (400 μm thick Ternophase). A borosilicate glass Petri dish (140 mm in diameter and 30 mm in height with 1 mm in thickness) containing the insects, was placed under the center of the active electrode, over the polyester films, thus contributing to the dielectric barrier. A needle-array electrode was employed to provide maximum exposure of the insects to the plasma. The gap between the bottom surface of the Petri dish and the tip of the needles (tip radius 50 μm) was fixed to 6 mm during the experiments. The high-voltage electrode was connected to a low-frequency (50 Hz) sine AC power supply (0–25 kV). The discharge was operated in open air. Oxygen or nitrogen were injected into the discharge active region as carrier gases with a measured gas-flow rate of 6 NL min^{-1}. The AC voltage applied to the needle-array electrode was measured by using a high-impedance voltage probe (Tektronix P6015A, 1000X, 3pf, 100 MHz) and displayed in a 4–channel oscilloscope (Tektronix TDS, 2004C with a sampling rate of 1 GS/s and an analogical bandwidth of 70 MHz). The power consumed by the discharge was inferred by using the method of the Lissajous figure, obtained by plotting the transported electric charge through the discharge (measured from the voltage drop across a measuring serial capacitor of 1.0 μF) as a function of the applied periodical voltage (Pipa et al., 2012). In addition, UV optical absorption

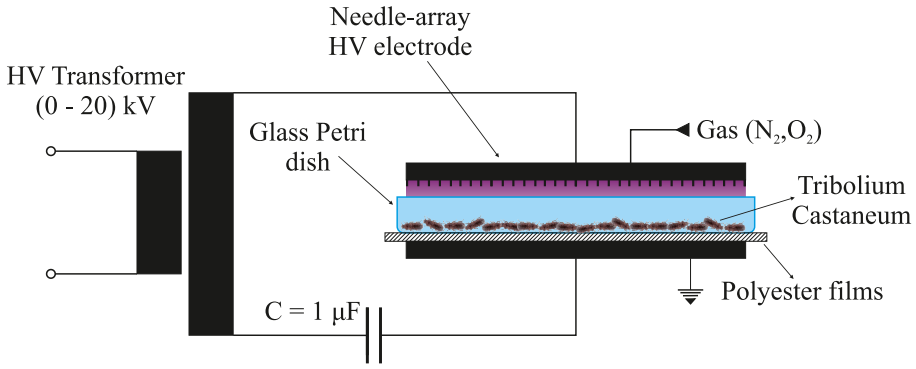

Fig. 1. Schematic of the experimental setup.

spectroscopy (OAS) was used to assess time-resolved ozone concentration in the discharge (Moiseev, 2014). The OAS was performed using a 254 nm UV line emitted by a mercury lamp (AVANTES, AvaLight-CAL). The point light source was constructed by focusing the UV light through a concentrating quartz lens (focal length 20 mm) on a pinhole with a 400 μ m diameter. The pinhole was placed in the focal point of the first biconvex quartz lens (focal length of 100 mm), which creates the collimated light test region of the OAS system. After passing through the test region in which the DBD was placed, the UV light was collected by a second biconvex quartz lens (focal length of 100 mm) and then focused onto the entrance slit of a monochromator (OBB $f = 200$ mm $f/4$,1200 l/mm) with 0.8 nm resolution. A photomultiplier (Hamamatsu R6350) attached to the monochromator was used to convert the light signal into an electrical signal, which was displayed in a 2–channel oscilloscope (Tektronix TDS 1002 B with a sampling rate of 500 MS/s and an analogical bandwidth of 60 MHz). The intensity of UV light at 254 nm was used to calculate ozone density based on Beer's law. The photoabsorption cross-section used was 1.15×10^{-21} m^2 (Daumont et al., 1992). The optical path length was the overall diameter of the high–voltage electrode (135 mm). The time resolution and detection limit of the OAS method were <1 s and <10 ppm, respectively. The experiments were conducted in ambient conditions (20 ± 1 °C and 45 ± 5% r.h.).

The obtained Lissajous figures are shown in Fig. 2.

As expected, the power consumed by the discharge for both gases decreased as the number of polyester films increased due to the decrease of the capacitance of the dielectric barrier (the capacitance of the air gap remained constant during the experiments). The specific power density was in the range of 0.13–0.32 W/cm^2. It was also observed that the power of the discharge, as well as the charge transferred through the gas (Q_{max}), were higher for nitrogen than for oxygen; which means that more microdischarges are initiated per unit of time and unit of electrode area. This behavior could be related to a decrease in the electron attachment as the oxygen content in the discharge decreases.

Fig. 3 shows time evolution profiles of ozone density under different discharge conditions. The amplitude of the applied voltage was 25 kVpp. The error bars are the standard deviation of data from different experimental sets. It was observed that the ozone density increased rapidly in the first seconds and reached a steady state at times greater than 30 s, independent of the type of gas and the number of polyester films of the barrier. However, the steady-state density values measured for oxygen were about 250% higher than that corresponding to nitrogen for the

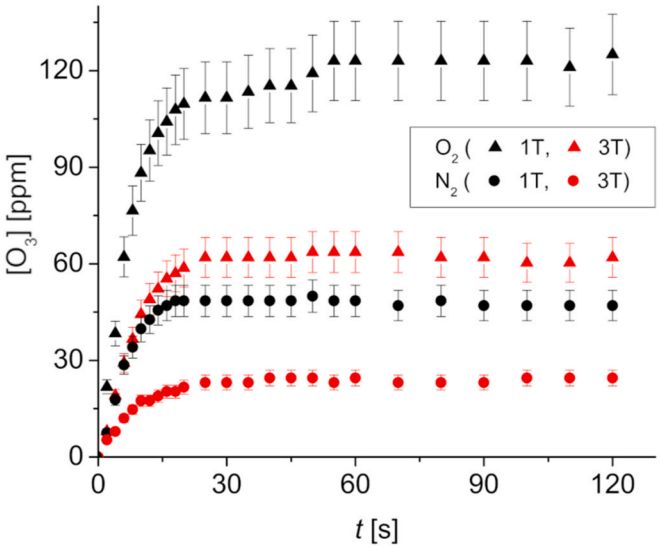

Fig. 3. Time evolution of ozone density under different discharge conditions.

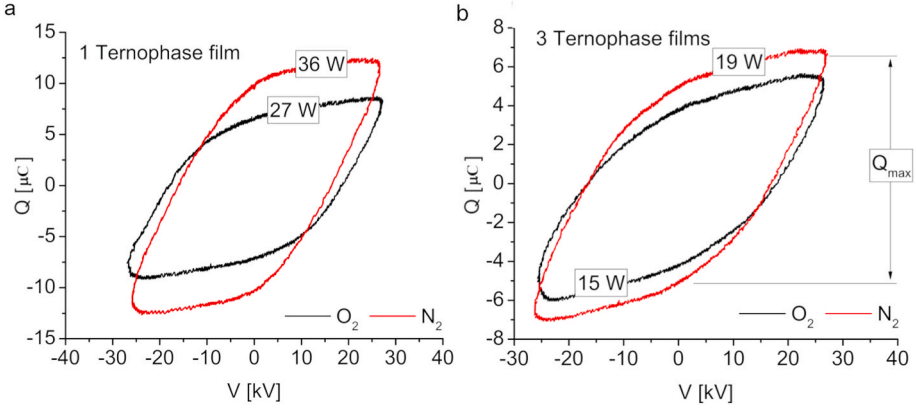

Fig. 2. Lissajous figure of the DBD for both carrier gases with a barrier of 1 Ternophase film (a); and 3 Ternophase films (b).

same barrier, showing that the ozone generation by the DBD increased markedly with the increase of O_2 content in the discharge. The ozone density for both gases increased as the power of the discharge increases (or when the number of polyester films decreases) under the conditions considered.

A preliminary screening was carried out to set up plasma conditions. Three biological replicates containing 20 larvae or 25 adults each, were subjected to plasma from 30 to 240 s, using 4 Ternophase layers and either O_2 or N_2 as a carrier gas.

Then, four treatments were selected: O30 (O_2, 30 s); O60 (O_2, 60 s); N30 (N_2, 30 s); N60 (N_2, 60 s). The untreated population remained as control (C). For all further experiments, 1 or 3 Ternophase films (1T and 3T, respectively) were employed. For each condition, five biological replicates with 30 larvae or 50 adults were used.

2.3. Mortality

Mortality in larvae and adults was checked at 1, 2 and 7 days after treatment. The mortality percentage was calculated according to Abbott (1925). Each individual was considered dead when a total absence of movement was observed.

2.4. Ovicidal activity

Fifty mixed-sex adults were kept in 1500 g of previously frozen wheat flour. After 5 days, the adults were removed and, for each replicate (n = 3), 60 g of sieved flour containing eggs, were placed in a Petri dish and were subjected to the following conditions: O3m3T (O_2, 3min, 3 Ternophase layers); O1m3T (O_2, 1min, 1 Ternophase layer); O3m3T (O_2, 3min, 3 Ternophase layers); N3m3T (N_2, 3min, 3 Ternophase layers); N1m1T (N_2, 1m, 1 Ternophase layer); N3m1T (N_2, 3min, 1 Ternophase layer). Afterward, the flour samples were incubated at the optimal rearing conditions and the number of larvae, pupae and adults was counted 3 and 12 weeks later.

2.5. Determination of moisture content

The moisture content of *T. castaneum* was measured with the oven method (Vogl and Ostermann, 2006).

2.6. Thiobarbituric acid reactive substances (TBARS) determination

Lipid peroxidation was measured as the amount of TBARS determined by the thiobarbituric acid (TBA) reaction as previously described by (Heath and Packer, 1968). Ten control and treated insects were homogenized in 1 ml of 20% (w/v) trichloroacetic acid (TCA). The homogenate was centrifuged at 10000×*g* for 20 min. To a 0.5 ml aliquot of the supernatant, 0.5 ml of 20% TCA containing 0.5% (w/v) TBA and 0.05 ml 4% butylated hydroxytoluene (BHT) in ethanol was added. The mixture was heated at 95 °C for 20 min and then quickly cooled on ice. The contents were centrifuged at 10000×*g* for 15 min and the absorbance was measured at 532 nm. The value for non-specific absorption at 600 nm was subtracted. The concentration of TBARS was calculated using an extinction coefficient of 155 mM^{-1} cm^{-1}. For each condition, three biological replicates were used.

2.7. Enzyme assays

Ten whole-body insects were ground and homogenized with 1 mg polyvinylpyrrolidone (PVP) in 1 ml of 50 mM phosphate extraction buffer (pH 7.7) containing 0.5 mM EDTA. The homogenate was centrifuged for 20 min at 10000 g at 4 °C. The activity of glutathione-S-transferase (GST) towards the substrate 1-Chloro-2,4-Dinitrobenzene (CDNB) was assayed according to (Vontas et al., 2000). Catalase (CAT) activity was determined in the homogenates by measuring the decrease in absorption at 240 nm in a reaction medium containing 50 mM potassium phosphate buffer (pH 7.2) and 2 mM H_2O_2 (Chance et al., 1979). Total superoxide dismutase (SOD) activity was determined by the inhibition of the photochemical reduction of NBT, as described by Becana et al. (1986). For each condition, five biological replicates of ten insects were used.

2.8. Atomic force microscopy

For Atomic force microscopy (AFM) measurements, we used three control samples and three different samples were treated and observed in three different zones. Both treated and control insects were superficially delipidized (to extract the cuticular lipids) by washing 5 min with hexane and then fixed in glass with buffer phosphate. All measurements were obtained immediately after fixation with Tapping mode in air, using probes doped with silicon nitride (RTESP, Veeco with tip nominal radius of 8 ± 12 nm, 271 ± 311 kHz, force constant 20 ± 80 N/m) using a MultiMode Scanning Probe Microscope (Veeco) equipped with a Nanoscope V controller (Veeco). The analysis was performed on two different areas, i.e. 15 μm^2 and 5 μm^2. The AFM measurements were acquired in the three different modes: height, for topographic determination; phase, to determinate possible change in the interaction for tip with the sample, and amplitude, to highlight small change topographic.

Roughness analysis: The effect of the treatments was analyzed on surface roughness using AFM and taking into consideration the Ra, Rq and Surface Area Difference values as quantitative parameters. The parameter Ra is the arithmetic mean of the deviations in height from the roughness mean value, Rq is the root mean square of the height distribution, and Surface Area Difference, is the difference between the analyzed three-dimensional area and its two-dimensional area. AFM image and data analysis were performed using the Nanoscope 7.30 and Nanoscope Analysis 1.5 software package.

2.9. Analysis of volatile organic compounds (VOCs) by solid phase microextraction coupled to capillary gas chromatography (SPME-CGC)

The volatile collections from both plasma-treated and control adults were performed with a 75-μm film thickness carboxen/polydimethylsiloxane (CAR/PDMS) (Supelco, Bellefonte, USA). The fiber was previously conditioned according to the manufacturer's instructions and systematically reconditioned before each analysis. Volatile organic compounds were sampled from live and dead adults, one day after treatment with different time exposures to O_2 or N_2 plasma, and controls. For each condition, five adults were placed in a 4 ml glass vial sealed with a Teflon cover with a rubber septum. The vial was heated at 90 °C for 15 min to release the totality of VOCs contained internally in insect glands (Villaverde et al., 2007); then VOCs were sampled immediately from the headspace (HS) corresponding to the gaseous phase in contact with the insect sample by SPME (Arthur and Pawliszyn, 1990). Five independent repetitions were performed for each condition. Vials containing no insects were used as blank controls. VOC analysis was performed by desorbing the fiber content in a Hewlett-Packard 6890 gas chromatograph equipped with a non-polar DB-5 capillary column (30 m length, 0.32 mm i.d., 0.25-μm film thickness) (J&W, Folsom, CA). The injector was operated in the splitless mode at 250 °C. The oven temperature was programmed from 40 °C for 1 min, 20 °C/min to 250 °C, with a holding time of 10 min at the final temperature. The flame ionization detector temperature was set at 280 °C. The peaks were identified by estimation of the Kovats retention index (KI) and their comparison with previous data from insect volatiles analyzed in the same conditions (Pedrini et al., 2010; Villaverde et al., 2009). VOCs peak areas were calculated for each chromatogram and expressed as a percentage of the total peak area detected by the fiber.

2.10. Statistical analysis

All data presented correspond to the mean value ± standard

deviation (SD) of the correspondent number of replicates. Analyses were performed using the statistic software package RCommander version 3.1.2 (2014). The variance ($p < 0.05$) of data was analyzed by one-way analysis of variance (ANOVA), after testing for the assumption of the normal distribution (Shapiro-Wilk's test) and homogeneity of variances (Levene's test). Tukey's HSD (Honestly-significant-difference) tests were performed for multiple comparisons of groups by means ($p < 0.05$).

3. Results

3.1. Insecticidal and ovicidal activity depends on the number of layers and exposure time

A first screening was carried out to test the efficacy of the DBD plasma arrangement in controlling the *T. castaneum* population. In these experimental conditions, four Ternophase layers were employed. Adults were exposed to plasma treatments from 30 to 240 s, using either O_2 or N_2 as carrier gases (Fig. 4a).

Twenty-four hours after the oxygen PNT treatments, the mortality percentage ranged from 14% to 55.6% by increasing time exposure, while higher values were obtained by changing the feed gas to nitrogen (from 24% to 72%). Two days after treatment (DAT), the percentage was raised to 92% with the longest N treatment (Fig. 4, middle panel). After seven days (Fig. 4, upper panel), O240, N120 and N180 treatments reached mortality values of 97%, 98% and 100%, respectively. After this pre-screening assay to set up the experimental conditions, the number of polymer layers was reduced to increase the power of discharge and improve beetle mortality (Fig. 2). To this aim, adults were exposed for 30 and 60 s to both gases, using either 1 or 3 polymer films.

As can be seen in Fig. 4b, after 24 h (lower panel), high levels of mortality were reached for each applied treatment, when a single layer (1T) was employed. However, 2 DAT these differences were significant only under the O30 condition, while in the remaining treatments, the percentage of killed insects was the same, despite how many layers were used.

The same conditions were carried out on the larval population. The results show that this life stage was more sensitive to all treatments (O30, O60, N30 and N60), achieving a 100% mortality (Fig. 5). No differences were observed respect to number of layers. Even shorter treatments were tested (10–15 s with one film layer) and the results remained unchanged (data not shown). Since eggs, unlike larvae, pupae and adults, are not visible to the naked eye, it is difficult to remove them from flours and grains. To test the ovicidal activity of NTP, 60 g of egg-containing flours were evaluated at three and twelve weeks after treatments. We carried out the experiments using 1 and 3 polymer layers. In addition, we also extended the time exposure to 1 and 3 min.

Three weeks after exposure (Fig. 6a, left white panel), 18 larvae, 1 to 5 pupae and no adults were found in each replicate of the untreated flours. Total number of larvae were drastically reduced in all treatments, dropping 78% under O3m3T and O1m1T conditions, 94.4% with N3m3T and N1m1T, while no larvae were found in N3m1T-treated flours. Concerning the other life cycle stages, just one pupa was observed in one of the O3m3T replicates, while neither pupae nor adults were found in the remaining treatments. Although these results seemed encouraging at first, 9 weeks later, the prospect changed significantly (Fig. 6a, right grey panel). The number of larvae, pupae and adults in

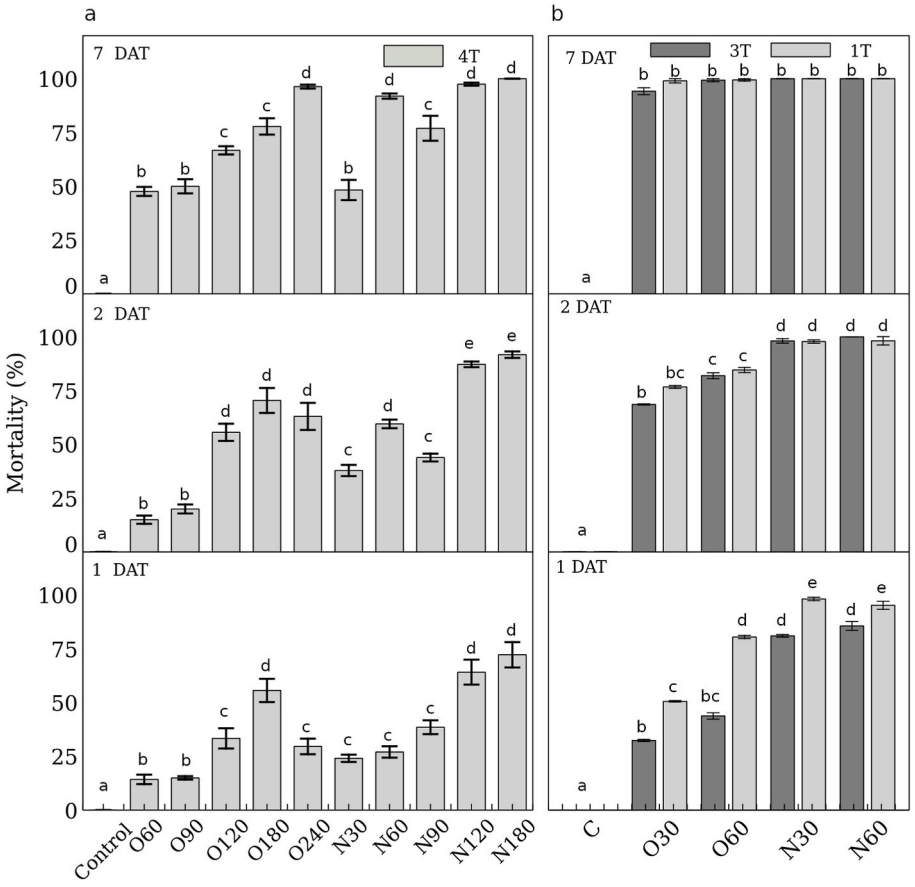

Fig. 4. Effects of carrier gases and time of exposure on mortality population of adult *T.castaneum* working with (a) 4, (b) 3 and 1 polymer layers. 4T, 3T and 1T refer to 4, 3 and 1 polymer layers, respectively. O and N refers to oxygen and nitrogen treatments, respectively. 30 to 240 refers to seconds of exposure to plasma. Error bars indicate standard deviation ($n = 3$, for 4T; $n = 5$, for 3T and 1T). Different letters indicate significant differences ($P < 0.05$) according to Tukey's multiple range test.

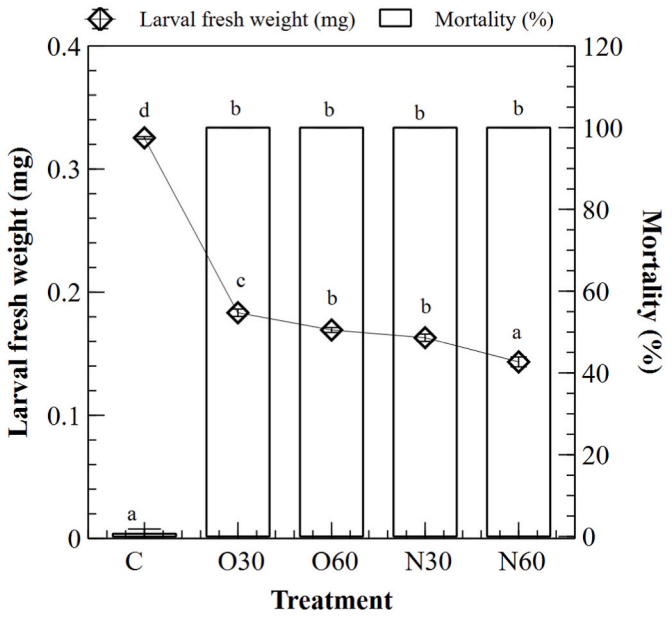

Fig. 5. Effects of carrier gases and time of exposure on viability and fresh weight of larvae population. Bar chart refers to mortality percentage and diamond symbols refer to larval fresh weight. O and N refers to oxygen and nitrogen treatments, respectively. 30 and 60 refers to seconds of exposure to plasma. Error bars indicate standard deviation (n = 3). Different letters indicate significant differences ($P < 0.05$) according to Tukey's multiple range test.

control samples were 108, 0 and 50, respectively. The larval counting in O3m3T and O1m1T flours was 12% and 11% lower than control, respectively, while it decreased by 90% in O3m1T treatment. All nitrogen-treated samples showed about a 98–100% reduction. Regarding pupae, one pupa was counted in just one of the replicates of both O3m3T and N1m1T flours. Except for the O1m1T treatment, where no differences were observed with respect to control, a significantly decreased number of adults was found in all treated flour, mainly on those subjected to nitrogen, with values diminished between 98.6% and 100% compared to control samples. Taking into account these results, we identified N3m3T as an ovicidal treatment, while the remaining NTPs partially killed the eggs and delayed the development of the life cycle. Due to restrictions imposed by pandemic COVID-19, some of these flour samples remained for more than 12 months in the chamber. Image in Fig. 6b shows their appearance. Interestingly, the flour took on a pinkish color for the control and O1m1T treatments, but remained white for the other more aggressive treatments.

3.2. Mortality is related to insect water content loss and redox imbalance

By analyzing the treated population, we found a significant reduction in fresh weight (FW) in both larvae and adults (Figs. 5 and 7, respectively). Fresh body weight decreased between 9% and 21% compared to the untreated population. The largest drop was observed with N60 treatment. In addition, the water loss also intensified as plasma exposure time increased, and under nitrogen presence. The water content in control insects was 55%, but dropped to 37% and 31% in those exposed to O30 and O60 treatments, respectively, while it lowered to 27% when nitrogen was employed as carrier gas. Regarding the larval stage, similar but enhanced results were observed: FW dropped between 44% and 56% compared to control, as time of exposure and power discharge increased.

While it is true that the discharge power is greater in the presence of nitrogen, it is not enough to explain the higher levels of mortality achieved. Therefore, in the next steps we focused on those treatments that will guarantee further studies on some physiological and biochemical responses of the survivors. Hence, since all the treatments employed

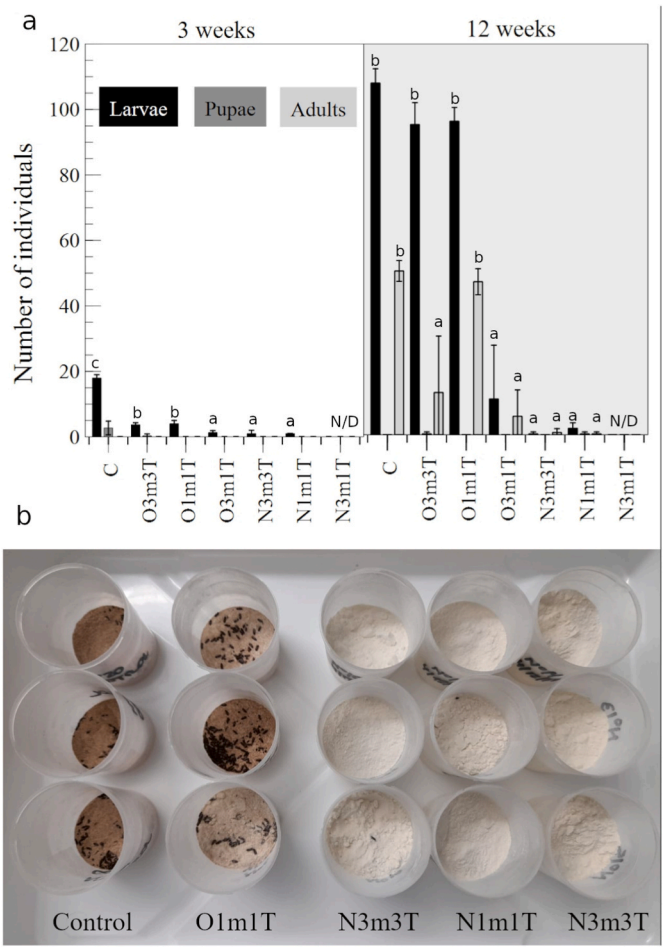

Fig. 6. Evaluation of the ovicidal properties of non-thermal plasmas on egg-containing wheat flour at three and 12 weeks (a) and 12 months (b) post-treatments. O3m3T (O_2, 3min, 3 Ternophase layers); O1m3T (O_2, 1min, 1 Ternophase layer); O3m3T (O_2, 3min, 3 Ternophase layers); N3m3T (N_2, 3min, 3 Ternophase layers); N1m1T (N_2, 1m, 1 Ternophase layer); N3m1T (N_2, 3min, 1 Ternophase layer). Error bars indicate standard deviation (n = 3). Different letters indicate significant differences ($P < 0.05$) according to Tukey's multiple range test.

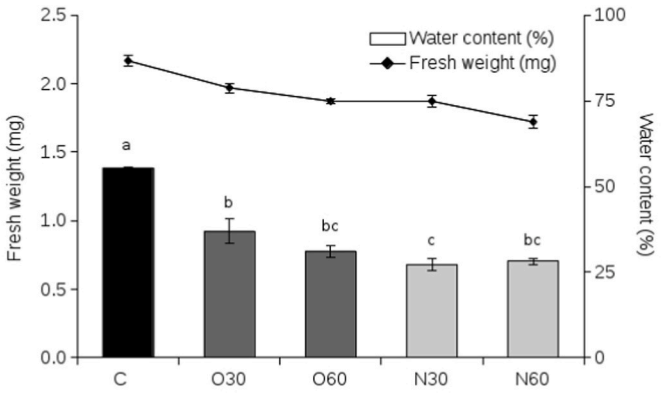

Fig. 7. Effects of different plasma treatments on fresh weight and water content of adult population. O and N refers to oxygen and nitrogen treatments, respectively. 30 and 60 refers to seconds of exposure to plasma. Error bars indicate standard deviation (n = 3). Different letters indicate significant differences ($P < 0.05$) according to Tukey's multiple range test.

killed 100% of larvae, only adults were analyzed.

It has been extensively reported that reactive oxygen species (ROS) are key components of the plasma (Adamovich et al., 2022; Misra et al., 2015). Therefore, we measured lipid peroxidation, an early marker of oxidative damage, in whole body insect extracts (Fig. 8a). As expected, this parameter also showed a time-and-gas-related injury. TBARS content increased 44% in the population subjected to O30 conditions and 65% in those treated with O60 and N30, while N60 triggered a 2.1-fold increase, respect to control. A plasma-triggered lipid peroxidation was also reported by Ziuzina et al. (2021).

Interestingly, we could not detect either reduced glutathione (GSH) or its oxidized form (GSSG) by the classic recycling method, even in the control insects (data not shown). This could be due to conjugation reactions between glutathione and the characteristic benzoquinones found in this specie, catalyzed by glutathione S-transferase (GST). GST activity (Fig. 8b) was induced by all the treatments applied, showing increases between 52% and 82% with respect to its control value (50 U.min^{-1}.mg^{-1}).

In addition to GST, the enzymatic activities of SOD and CAT were also determined. We found an induced CAT activity (Fig. 8c), but a lower SOD activity compared to untreated beetles (Fig. 8d).

3.3. Oxygen and nitrogen NTP treatments provoke different damage on the insect surface and cuticular secretions

To find effects other than oxidative damage that could explain why nitrogen increases mortality, we decided to explore the surface of untreated adult beetles and those submitted to O60 and N60 conditions. The prothorax segment surface has a fairly conserved pentagonal and hexagonal structure with numerous glands that produce and secrete chemical compounds on the surface. The effect of the treatments was analyzed on the surface roughness of the prothorax segment using the AFM technique, on a 15-μm section length. The AFM provides a 3D profile on a nanoscale, by measuring forces between a sharp probe and surface at very short distance (0.2–10 nm). The probe is supported on a flexible cantilever and the AFM tip touches

the surface and records the small force between the probe and the surface. As can be seen in Fig. 9, despite the shape of the units being preserved, oxygen and nitrogen discharges provoked the loss of the curvature and modified the space between the units affecting the normal compact structure of the tissue observed in untreated samples. Although the roughness values Ra and Rq are the most widely used values in surface analysis, according to their definition, these parameters are based on the difference in profile with respect to a mean line, and depending on the characteristics of the surfaces, may not discriminate between samples. That is why other characteristics of the surface must be used, in our case the Area Difference, which is the difference of the total area (sum of the area of all the triangles formed by three adjacent data points) and the area in two dimensions of the analyzed region. Visually, in Fig. 9 it would be the sum of the differences of the maximum length of each line with respect to the length of the white line (in our example, 15 μm). In particular, the aggressiveness of the nitrogen treatment was evidenced by the 2.5-fold increase of the Surface Area Difference parameter (1.96 vs. 4.96, blue circles in the small plot,

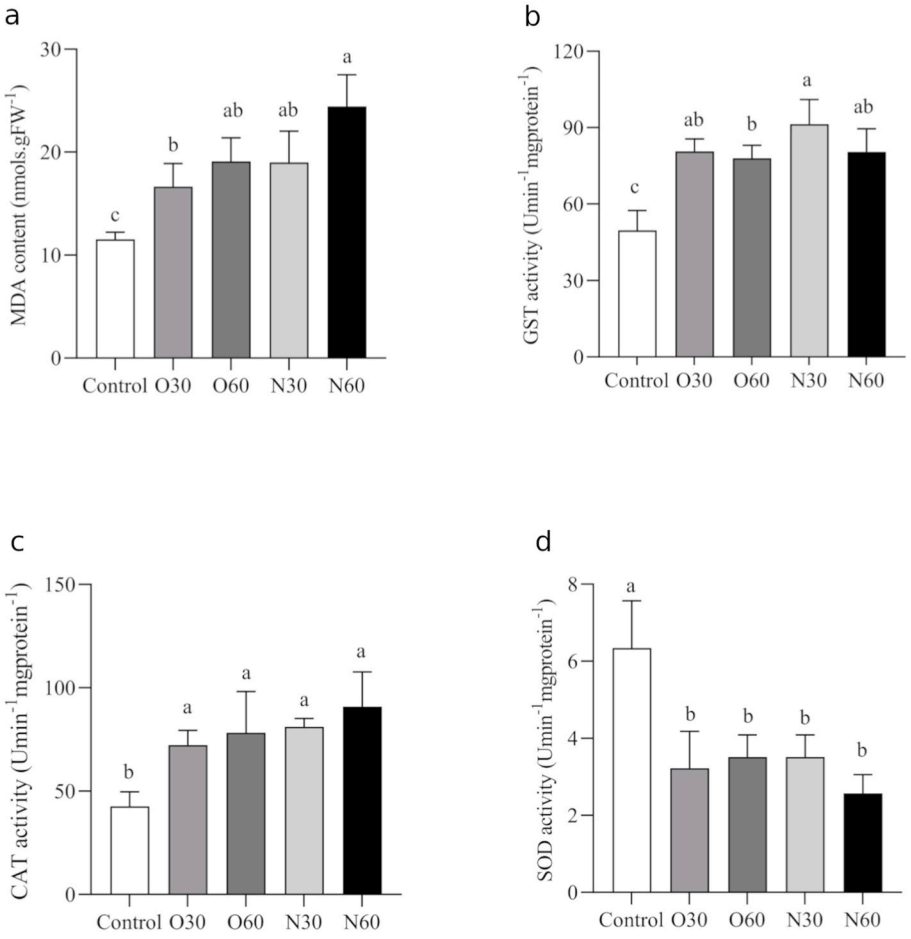

Fig. 8. Effects of plasmas on lipid peroxidation (a) and enzymatic antioxidant response (b–d). O and N refers to oxygen and nitrogen treatments, respectively. 30 and 60 refers to seconds of exposure to plasma. Error bars indicate standard deviation (n = 3, for lipid peroxidation; n = 5, for enzyme activities). Different letters indicate significant differences ($P < 0.05$) according to Tukey's multiple range test.

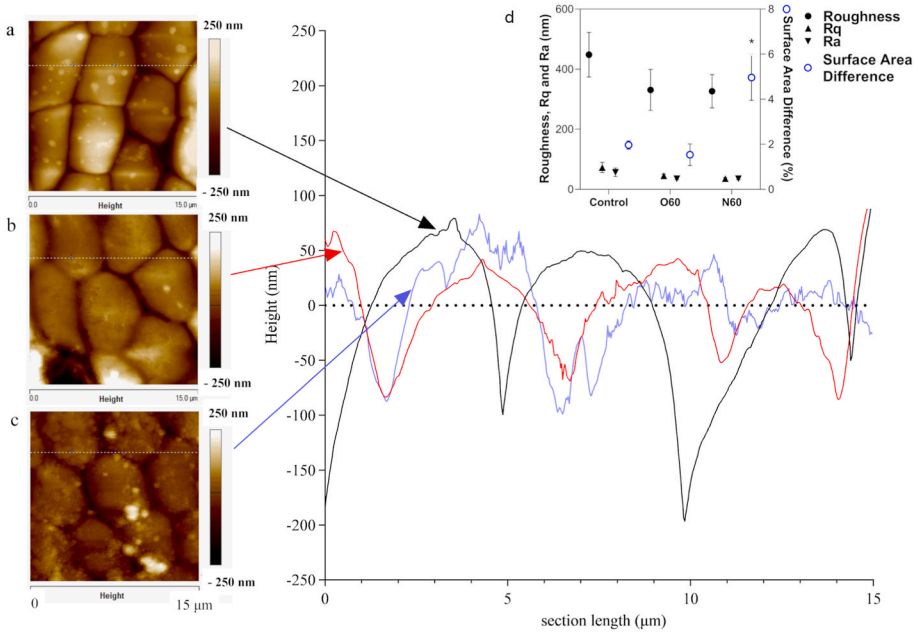

Fig. 9. Impact of carrier gases on the cuticular surface of *T. castaneum.* Images and plots show the scan of prothorax surface of the untreated (a, black line) insects, and those exposed to oxygen (b, red line) and nitrogen (c, blue line) plasma treatments. The upper small plot (d) shows the AFM parameters. Asterik indicate significant differences ($P < 0.05$) according to Tukey's multiple range test.

Fig. 9d). In contrast, because of the large scattering of the data obtained from the O60 treatment, its AFM parameters did not differ statistically from the control (Fig. 9d).

As a consequence of the cuticle damage, the quinone-containing secretions of the prothoracic and abdominal glands were also affected (Fig. 10). The main benzoquinones, ethyl-1,4-benzoquinone (EBQ) and methyl-1,4-benzoquinone (MBQ), were semi-quantified by solid phase micro-extraction coupled to capillary gas chromatography (SPME-CGC), in both live and dead insects. In the former group, N30 treatments showed a significant reduction in the quantities of both EBQ and MBQ

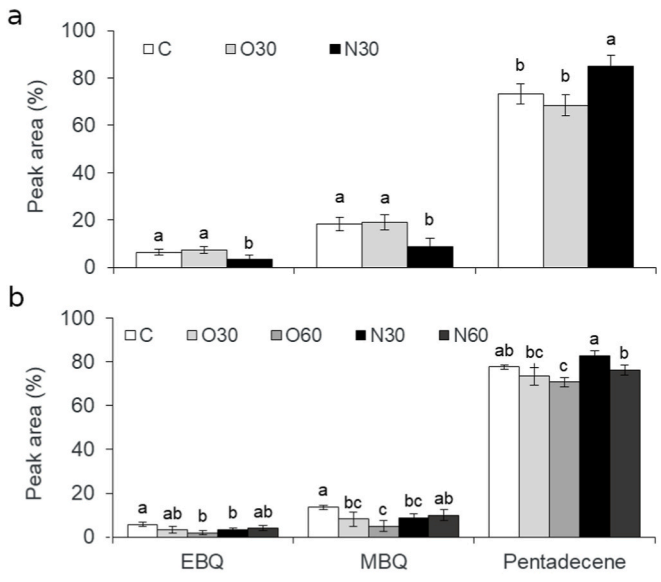

Fig. 10. Effects of plasma treatments on the quinone-secretion of the prothoracic and abdominal glands of live (a) and dead (b) adult population. The main benzoquinones analyzed were ethyl-1,4-benzoquinone (EBQ) and methyl-1,4-benzoquinone (MBQ). Error bars indicate standard deviation (n = 5). Different letters indicate significant differences ($P < 0.05$) according to Tukey's multiple range test.

detected in the headspace compared with control insects ($p < 0.05$); however, no significant changes were detected in O30 treatments. Regarding dead insects, the reduction in benzoquinones was evident also for oxygen discharges, with significant differences found in both EBQ and MBQ detection ($p < 0.05$).

4. Discussion

Other authors have previously pointed out that NTPs are an effective tool in the control of insect pests. In this work, we provided further evidence in this regard.

The insecticidal activity of our DBD plasma against eggs, larvae and adults of *T. castaneum* was highly influenced by exposure times (30–240 s), carrier gas (O_2 or N_2) and power of discharge (1–4 polymer layers). In general, better results were always obtained using one Thernofase layer and nitrogen as working gas. It has been reported that plasma is a source of ozone and reactive species of oxygen and nitrogen, which are responsible for the oxidative damage triggered (Adamovich et al., 2022; Misra et al., 2015). The steady state density of ozone measured for oxygen is about 250% higher than that corresponding to nitrogen (Fig. 3); thus, suggesting that ozone does not seem to play a relevant role in insect mortality under the conditions considered. These findings reinforce previous work exploring the use of ozone in pest control, where lower mortality rates were reported in adults and larvae after exposure to 40 ppm for 24 and 6 h, respectively (Holmstrup et al., 2011). By using just air as feed gas, Ziuzina et al. (2021) tested the effects of direct and indirect exposure to plasmas. They also reported 100% mortality levels after 24 h in eggs, larvae and pupae. In contrast to our results, they found an adult lethality close to 20% after 1-min treatment, but working in the presence of flour and grains that could have attenuated the impact of the discharge. Ratish Ramanan et al. (2018), explored the influence of voltage, exposure time (up to 20 min) and electrode gap (2-6-cm between electrodes), on the mortality of insects, reaching values that ranged between 0 and 100%. Their samples were treated inside a chamber operated at low-pressure (about 1 mbar), and therefore at higher costs and greater complexity compared to our method proposed here.

Working under our prototype conditions, we identified a 1-min

nitrogen treatment that prevents the emergence of larvae, pupae and adults from egg-infested flour, until 12-month post-treatment, avoiding chemical residues and the emergence of resistant populations. The pink coloration observed in untreated flour and those subjected to oxygen is a sign of the benzoquinones released by the glands of adult insects. Nitrogen-treated samples remained white. This last result highlighted the ovicidal properties of nitrogen treatments and strongly suggest that NTPs could be powerful tools in controlling insects and preserving flour quality. However, further experiments should be carried out to obtain a detailed nutritional composition and rheological properties of dough of treated flour. In this regard, the effects of NTPs on the functional and structural properties of sealed pack flours were previously explored by Misra et al. (2015). Working under moderate voltage (60 and 70 kV) by 5 and 10 min, they found voltage and time-related changes in elasticity and viscosity and also revealed the alteration of the secondary structure of gluten proteins following NTP exposure. The authors concluded that the observed changes were the result of the action of reactive species present in NTPs.

In contrast to plasma-triggered lipid peroxidation which increases as treatments intensify, the antioxidant response capacity was already exceeded by the O30 treatment, since all enzyme activities were statistically different from the untreated population, while (almost) no differences were registered among them.

A similar profile of stress-marker enzymes was reported by other authors in *T. castaneum*, as a response against two pro-oxidant insecticides: pirimiphos-methyl and deltamethrin (Plavšin et al., 2015). While we would have expected a high SOD activity, our results showed a lower activity that might be the result of an H_2O_2-mediated inhibition. In fact, it is well known that high concentrations of H_2O_2 inhibit the activity of SOD *in vivo* (Hodgson and Fridovich 1975; Gottfredsen et al., 2013). Winter et al. (2014) tracked and quantified the H_2O_2 generation in the plasma gaseous phase, by an atmospheric pressure plasma jet, to its transition into the liquid phase. Therefore, we hypothesized that the high levels of H_2O_2 generated in plasma provoke the activation of CAT, but the inhibition of SOD by an end-product mechanism.

It is interesting to note that Ziuzina et al. (2021) reported also an increased GST activity, while no changes were observed in CAT and SOD activity. This contrasted behavior could be explained by the use of working gases with difference in chemical composition.

Reactions between GSH as well as its radical forms, $GS^{\bullet}$ and $GSSG^{\bullet-}$, with benzoquinones were described in detail by Butler and Hoey (1992). In insects, GST primarily metabolizes lipid peroxides (Vontas et al., 2000), but has a wide range of substrate specificity such as organic hydroperoxides, quinones, and carbonyls. Therefore, the increased GST activity observed is likely related to its dual role in neutralizing the byproducts of lipid peroxidation and forming GSH–quinone adducts.

The intensity of the cuticle damage produced by each treatment could also explain the difference in water loss and mortality levels. In particular, the disruption of the cuticle lipid layer can result in dehydration and insect mortality (Hassan et al., 2020). Dehydration observed is typically associated with the action of plasma-generated species on the insect tissue (Ratish Ramanan et al., 2018).

AFM was employed previously to study and quantify 3D structures of nano-arrays of the surface of different insects (Watson and Blach, 2002). The marked morphological changes found in the AFM scanning of the insect cuticle could be due to charge accumulation on the surface, which induces an electrostatic pressure that can overcome the tensile strength of the insect tissue, leading to its disruption. Cellular destruction through plasma etching effects can also play a role (Bourke et al., 2017; Bures et al., 2006).

The reduction in EBQ and MBQ content is in coincidence with the results obtained by AFM, in which nitrogen discharges resulted more aggressively for the insect surfaces than oxygen discharges. Previous reports showed that the volatiles released by *T. castaneum* decreased around 20% after infection with an entomopathogenic fungus (Davyt-Colo et al., 2022; Pedrini et al., 2010). In this study, the 2-fold diminution of benzoquinones secretion in N30 treatment compared to controls is in concordance with the more aggressive treatment (measured by both mortality and surface damage) caused by plasma discharges in comparison with the effect of pathogenic fungi. Since the secretion of volatiles depends on the nervous system, dead insects cannot secrete them; therefore, the observed effect might be since cadavers, having damaged their cuticular surface by both types of discharges, have lost much benzoquinones due to volatilization before the sampling by SPME.

The highest mortality rate was achieved by using nitrogen as a carrier gas, since it causes more severe structural and oxidative damage on the insect surface, in comparison to oxygen, leading to increased dehydration and loss of benzoquinones. Just a few seconds to direct exposure to plasma killed adults and larvae, while it took longer times in controlling the egg stage probably due to interference caused by the flour. Besides the shorter times, nitrogen presents other advantages over the use of oxygen: it is less expensive and the ozone production is considerably lower, improving operational conditions and costs.

Although the above-described experiments have been carried out on a laboratory scale, this plasma-based technology could be scaled up through a parallel arrangement of DBDs in order to meet practical technological applications. For instance, for post-harvest pest management, this technology can be applied by exposing the infected commodities to NTP through a large-scale reactor, before to packaging for storage.

Funding

This work was supported by grants from: Universidad Tecnológica Nacional (PID 8461), Agencia Nacional de Promoción Científica y Tecnológica (PICT 2018 N 702) and Universidad de Buenos Aires (UBACYT, 20020190100043BA).

Credit authorship contribution statemen

CZ: Investigation, Methodology, Formal analysis, Data curation, Writing – original draft. **NP:** Methodology, Formal analysis, Data curation. Writing – review & editing. **EP:** Methodology, Formal analysis, Data curation. Writing – review & editing. **JRG:** Methodology. **PV:** Methodology. **MF:** Methodology. **JCCh:** Methodology. **EC:** Methodology, Formal analysis, Data curation. **BF:** Methodology. **LP:** Supervision, Validation, Project administration. **KB:** Supervision, Validation, Project administration.

Declaration of competing interest

The authors declare that they have no known competing financial interests or personal relationships that could have appeared to influence the work reported in this paper.

Data availability

The data that has been used is confidential.

References

Abbott, W., 1925. A Method of Computing the Effectiveness of an Insecticide. J. Econ. Entomol. https://doi.org/10.1093/jee/18.2.265a.

Adamovich, I., Agarwal, S., Ahedo, E., Alves, L.L., Baalrud, S., Babaeva, N., Bogaerts, A., Bourdon, A., Bruggeman, P.J., Canal, C., Choi, E.H., Coulombe, S., Donkó, Z., Graves, D.B., Hamaguchi, S., Hegemann, D., Hori, M., Kim, H.-H., Kroesen, G.M.W., Kushner, M.J., Laricchiuta, A., Li, X., Magin, T.E., Mededovic Thagard, S., Miller, V., Murphy, A.B., Oehrlein, G.S., Puac, N., Sankaran, R.M., Samukawa, S., Shiratani, M., Šimek, M., Tarasenko, N., Terashima, K., Thomas Jr., E., Trieschmann, J., Tsikata, S., Turner, M.M., van der Walt, I.J., van de Sanden, M.C.M., von Woedtke, T., 2022. The 2022 Plasma Roadmap: low temperature plasma science and technology. J. Phys. D Appl. Phys. 55, 373001 https://doi.org/10.1088/1361-6463/ac5e1c.

Akbar, W., Lord, J.C., Nechols, J.R., Howard, R.W., 2004. Diatomaceous earth increases the efficacy of Beauveria bassiana against Tribolium castaneum larvae and increases

conidia attachment. J. Econ. Entomol. 97, 273–280. https://doi.org/10.1603/0022-0493-97.2.273.
Arthur, C.L., Pawliszyn, J., 1990. Solid phase microextraction with thermal desorption using fused silica optical fibers. Anal. Chem. 62, 2145–2148.
Becana, M., Aparicio-Tejo, P., Irigoyen, J.J., Sanchez-Diaz, M., 1986. Some enzymes of hydrogen peroxide metabolism in leaves and root nodules of Medicago sativa. Plant Physiol. 82, 1169–1171.
Bourke, P., Ziuzina, D., Han, L., Cullen, P.J., Gilmore, B.F., 2017. Microbiological interactions with cold plasma. J. Appl. Microbiol. https://doi.org/10.1111/jam.13429.
Brandenburg, R., 2017. Dielectric barrier discharges: progress on plasma sources and on the understanding of regimes and single filaments. Plasma Sources Sci. Technol. 26, 053001 https://doi.org/10.1088/1361-6595/aa6426.
Bruggeman, P.J., Iza, F., Brandenburg, R., 2017. Foundations of atmospheric pressure non-equilibrium plasmas. Plasma Sources Sci. Technol. 26, 123002 https://doi.org/10.1088/1361-6595/aa97af.
Bures, B., Donohue, K., Roe, R., Bourham, M., 2006. Nonchemical dielectric barrier discharge treatment as a method of insect control. Plasma Sci. IEEE Trans. 34, 55–62. https://doi.org/10.1109/TPS.2005.863595.
Butler, J., Hoey, B.M., 1992. Reactions of glutathione and glutathione radicals with benzoquinones. Free Radic. Biol. Med. 12, 337–345. https://doi.org/10.1016/0891-5849(92)90082-R.
Chance, B., Sies, H., Boveris, A., 1979. Hydroperoxide metabolism in mammalian organs. Physiol. Rev. 59, 527–605. https://doi.org/10.1152/physrev.1979.59.3.527.
Dasan, B.G., Mutlu, M., Boyaci, I.H., 2016. Decontamination of Aspergillus flavus and Aspergillus parasiticus spores on hazelnuts via atmospheric pressure fluidized bed plasma reactor. Int. J. Food Microbiol. 216, 50–59. https://doi.org/10.1016/J.IJFOODMICRO.2015.09.006.
Daumont, D., Brion, J., Charbonnier, J., et al., 1992. Ozone UV spectroscopy I: Absorption cross-sections at room temperature. J. Atmos. Chem. https://doi.org/10.1007/BF00053756.
Davyt-Colo, B., Girotti, J.R., González, A., Pedrini, N., 2022. Secretion and Detection of Defensive Compounds by the Red Flour Beetle Tribolium castaneum Interacting with the Insect Pathogenic Fungus Beauveria Bassiana. Pathog. https://doi.org/10.3390/pathogens11050487.
Donohue, K.V., Bures, B.L., Bourham, M.A., Roe, R.M., 2015. Mode of action of a novel nonchemical method of insect control: atmospheric pressure plasma discharge. J. Econ. Entomol. 99, 38–47. https://doi.org/10.1093/jee/99.1.38.
Faruki, S.I., Das, D.R., Khan, A.R., Khatun, M., 2007. Effects of ultraviolet (254nm) irradiation on egg hatching and adult emergence of the flour beetles, Tribolium castaneum, T. confusum and the almond moth, Cadra cautella. J. Insect Sci. 7 https://doi.org/10.1673/031.007.3601.
Fridman, A., Chirokov, A., Gutsol, A., 2005. Non-thermal atmospheric pressure discharges. In: Journal of Physics D: Applied Physics, pp. R1–R24. https://doi.org/10.1088/0022-3727/38/2/R01.
Gautam, S.G., Opit, G.P., Hosoda, E., 2016. Phosphine resistance in adult and immature life stages of Tribolium castaneum (Coleoptera: Tenebrionidae) and Plodia interpunctella (Lepidoptera: Pyralidae) populations in California. J. Econ. Entomol. 109, 2525–2533. https://doi.org/10.1093/jee/tow221.
Gottfredsen, R.H., Larsen, U.G., Enghild, J.J., Petersen, S.V., 2013. Hydrogen peroxide induce modifications of human extracellular superoxide dismutase that results in enzyme inhibition. Redox Biol. 1, 24–31. https://doi.org/10.1016/j.redox.2012.12.004.
Hajek, A.E., St Leger, R.J., 1994. Interactions between fungal pathogens and insect hosts. Annu. Rev. Entomol. 39, 293–322. https://doi.org/10.1146/annurev.en.39.010194.001453.
Hassan, A.M., Sileem, T.M., Hassan, R.S., 2020. Verification of atmospheric plasma irradiation as an alternative control method for tribolium castaneum (Herbst). Braz. J. Biol. 80, 673–679. https://doi.org/10.1590/1519-6984.222662.
Heath, R.L., Packer, L., 1968. Photoperoxidation in isolated chloroplasts. I. Kinetics and stoichiometry of fatty acid peroxidation. Arch. Biochem. Biophys. 125, 189–198. https://doi.org/10.1016/0003-9861(68)90654-1.
Hodgson, E.K., Fridovich, I., 1975. Interaction of bovine erythrocyte superoxide dismutase with hydrogen peroxide. Chemiluminescence and peroxidation. Biochemistry 14, 5299–5303. https://doi.org/10.1021/bi00695a011.
Holmstrup, M., Sørensen, J.G., Heckmann, L.-H., Slotsbo, S., Hansen, P., Hansen, L.S., 2011. Effects of ozone on gene expression and lipid peroxidation in adults and larvae of the red flour beetle (Tribolium castaneum). J. Stored Prod. Res. 47, 378–384. https://doi.org/10.1016/j.jspr.2011.07.002.
Jagadeesan, R., Collins, P.J., Daglish, G.J., Ebert, P.R., Schlipalius, D.I., 2012. Phosphine resistance in the rust red flour beetle, Tribolium castaneum (Coleoptera: Tenebrionidae): inheritance, gene interactions and fitness costs. PLoS One 7. https://doi.org/10.1371/journal.pone.0031582.
Khan, M., Ali, A., Memon, S.A., Qambrani, T.K., Khaliq, G., Khan, J., Ahmed, S., Abro, A. H., Baloch, S.A., 2021. Function of ultraviolet radiation (UV-B) light on the survival of red flour beetle Tribolium castaneum (herbst) (Coleoptera:Tenebrionidae) and their body fitness. Pakistan J. Agric. Res. 34, 748–757. https://doi.org/10.17582/journal.pjar/2021/34.4.748.757.
Khanzada, H., Sarwar, M., Lohar, M., 2015. Repellence activity of plant oils against red flour beetle Tribolium castaneum (Herbst)(Coleoptera: Tenebrionidae) in wheat. Int. J. Anim. Biol. 1, 86–92.
Kunhardt, E.E., 2000. Generation of large-volume, atmospheric-pressure, nonequilibrium plasmas. IEEE Trans. Plasma Sci. 28, 189–200. https://doi.org/10.1109/27.842901.
Lord, J.C., 2007. Enhanced efficacy of Beauveria bassiana for red flour beetle with reduced moisture. J. Econ. Entomol. 100, 1071–1074. https://doi.org/10.1603/0022-0493(2007)100[1071:eeobbf]2.0.co;2.
McDonough, M.X., Mason, L.J., Woloshuk, C.P., 2011. Susceptibility of stored product insects to high concentrations of ozone at different exposure intervals. J. Stored Prod. Res. 47, 306–310. https://doi.org/10.1016/j.jspr.2011.04.003.
Misra, N.N., Kaur, S., Tiwari, B.K., Kaur, A., Singh, N., Cullen, P.J., 2015. Atmospheric pressure cold plasma (ACP) treatment of wheat flour. Food Hydrocolloids 44, 115–121. https://doi.org/10.1016/j.foodhyd.2014.08.019.
Moiseev, T., 2014. Post-Discharge Gas Composition of a Large-Gap DBD in Humid Air by UV – Vis. https://doi.org/10.1088/0963-0252/23/6/065033.
Patil, H., Shejale, K.P., Jabaraj, R., Shah, N., Kumar, G., 2020. Disinfestation of red flour beetle (Tribolium castaneum) present in almonds (Prunus dulcis) using microwave heating and evaluation of quality and shelf life of almonds. J. Stored Prod. Res. 87, 101616 https://doi.org/10.1016/j.jspr.2020.101616.
Pedrini, N., Ortiz-Urquiza, A., Huarte-Bonnet, C., Fan, Y., Juárez, M.P., Keyhani, N.O., 2015. Tenebrionid secretions and a fungal benzoquinone oxidoreductase form competing components of an arms race between a host and pathogen. Proc. Natl. Acad. Sci. USA 112, E3651–E3660. https://doi.org/10.1073/pnas.1504552112.
Pedrini, N., Villaverde, M.L., Fuse, C.B., Dal Bello, G.M., Juárez, M.P., 2010. *Beauveria bassiana* infection alters colony development and defensive secretions of the beetles *Tribolium castaneum* and *Ulomoides dermestoides* (Coleoptera: Tenebrionidae). J. Econ. Entomol. 103, 1094–1099. https://doi.org/10.1603/ec10072.
Pérez-Pizá, M.C., Grijalba, P.E., Cejas, E., Chamorro Garcés, J.C., Ferreyra, M., Zilli, C., Vallecorsa, P., Santa-Cruz, D., Yannarelli, G., Prevosto, L., Balestrasse, K., 2021. Effects of non-thermal plasma technology on Diaporthe longicolla cultures and mechanisms involved. Pest Manag. Sci. 77, 2068–2077. https://doi.org/10.1002/ps.6234.
Pérez-Pizá, M.C., Prevosto, L., Grijalba, P.E., Zilli, C.G., Cejas, E., Mancinelli, B., Balestrasse, K.B., 2019. Improvement of growth and yield of soybean plants through the application of non-thermal plasmas to seeds with different health status. Heliyon 5. https://doi.org/10.1016/j.heliyon.2019.e01495.
Pipa, A.V., et al., 2012. The simplest equivalent circuit of a pulsed dielectric barrier discharge and the determination of the gas gap charge transfer. Rev. Sci. Instrum.
Plavšin, I., Stašková, T., Šerý, M., Smýkal, V., Hackenberger, B.K., Kodrík, D., 2015. Hormonal enhancement of insecticide efficacy in Tribolium castaneum: oxidative stress and metabolic aspects. Comp. Biochem. Physiol., Part C: Toxicol. Pharmacol. 170, 19–27. https://doi.org/10.1016/j.cbpc.2015.01.005.
Ratish Ramanan, K., Sarumathi, R., Mahendran, R., 2018. Influence of cold plasma on mortality rate of different life stages of Tribolium castaneum on refined wheat flour. J. Stored Prod. Res. 77, 126–134. https://doi.org/10.1016/j.jspr.2018.04.006.
Sahaf, Bibi, Zahra, et al., 2007. Chemical constituents and fumigant toxicity of essential oil from Carum copticum against two stored product beetles. Insect Sci. https://doi.org/10.1111/j.1744-7917.2007.00146.x.
Saroukolai, A.T., Moharramipour, S., Meshkatalsadat, M.H., Gautam, S.G., Opit, G.P., Hosoda, E., 2010. Insecticidal properties of Thymus persicus essential oil against Tribolium castaneum and Sitophilus oryzae. J. Pest. Sci. 109 (2004), 3–8. https://doi.org/10.1093/jee/tow221.
Şen, Y., Bağcı, U., Güleç, H.A., Mutlu, M., 2012. Modification of food-contacting surfaces by plasma polymerization technique: reducing the biofouling of microorganisms on stainless steel surface. Food Bioprocess Technol. 5, 166–175. https://doi.org/10.1007/s11947-009-0248-1.
Singh, S., Prakash, S., 2013. Development of resistance in Tribolium castaneum, Herbst (Coleoptera: Tenebrionidae) towards deltamethrin in laboratory. Int. J. Sci. Res. Publ. 3, 1–4.
Villaverde, M.L., Girotti, J.R., Mijailovsky, S.J., Pedrini, N., Juárez, M.P., 2009. Volatile secretions and epicuticular hydrocarbons of the beetle Ulomoides dermestoides. Comp. Biochem. Physiol. B Biochem. Mol. Biol. 154, 381–386. https://doi.org/10.1016/j.cbpb.2009.08.001.
Villaverde, M.L., Juárez, M.P., Mijailovsky, S., 2007. Detection of Tribolium castaneum (Herbst) volatile defensive secretions by solid phase microextraction-capillary gas chromatography (SPME-CGC). J. Stored Prod. Res. 43, 540–545. https://doi.org/10.1016/j.jspr.2007.03.003.
Vogl, J., Ostermann, M., 2006. On the measurement of the moisture content in different matrix materials. Accred Qual. Assur. 11, 356–362. https://doi.org/10.1007/s00769-006-0159-z.
Vontas, J.G., Enayati, A.A., Small, G.J., Hemingway, J., 2000. A simple biochemical assay for glutathione S-transferase activity and its possible field application for screening glutathione S-transferase-based insecticide resistance. Pestic. Biochem. Physiol. 68, 184–192. https://doi.org/10.1006/pest.2000.2512.
Watson, G., Blach, J., 2002. Characterisation of cuticular nanostructures on surfaces of insects by atomic force microscopy: mining evolution for smart structures. Smart Mater. II. https://doi.org/10.1117/12.469733.
Winter, J., Tresp, H., Hammer, M.U., Iseni, S., Kupsch, S., Schmidt-Bleker, A., Wende, K., Dünnbier, M., Masur, K., Weltmann, K.D., Reuter, S., 2014. Tracking plasma generated H2O2 from gas into liquid phase and revealing its dominant impact on human skin cells. J. Phys. D Appl. Phys. 47 https://doi.org/10.1088/0022-3727/47/28/285401.
Xinyi, E., Subramanyam, B., Li, B., 2017. Efficacy of ozone against phosphine susceptible and resistant strains of four stored-product insect species. Insects 8. https://doi.org/10.3390/insects8020042.
Yang, F.L., Li, X.G., Zhu, F., Lei, C.L., 2009. Structural characterization of nanoparticles loaded with garlic essential oil and their insecticidal activity against Tribolium castaneum (Herbst) (Coleoptera: Tenebrionidae). J. Agric. Food Chem. 57, 10156–10162. https://doi.org/10.1021/jf9023118.
Ziuzina, D., van Cleynenbreugel, R., Tersaruolo, C., Bourke, P., 2021. Cold plasma for insect pest control: Tribolium castaneum mortality and defense mechanisms in response to treatment. Plasma Process. Polym. 18, 1–12. https://doi.org/10.1002/ppap.202000178.